THE JOURNAL OF PHYSICAL CHEMISTRY LETTERS
A JOURNAL OF THE AMERICAN CHEMICAL SOCIETY

pubs.acs.org/JPCL Letter

Ultraviolet Photolysis of Acetaldehyde in Clathrate Hydrate Reveals Cage-Controlled Reactivity

Gaurav Vishwakarma, Soham Chowdhury, Rajnish Kumar,* and Thalappil Pradeep*

Cite This: https://doi.org/10.1021/acs.jpclett.6c00885 Read Online

ACCESS | Metrics & More | Article Recommendations | Supporting Information

ABSTRACT: Clathrate hydrates (CHs), crystalline inclusion compounds composed of hydrogen-bonded water cages, have been proposed to act as "tiny reaction vessels", potentially providing unique environments for chemical transformations. Although these cages can enable distinct photochemistry by stabilizing and retaining reactive species, the interactions of CHs with ultraviolet (UV) radiation remain understudied. Using reflection absorption infrared spectroscopy, we investigated the UV photochemistry and subsequent thermal processing of the acetaldehyde clathrate hydrate (ACH), comparing its behavior with that of pure acetaldehyde and acetaldehyde + H_2O mixed ices under ultrahigh vacuum ($\sim 10^{-10}$ mbar) and cryogenic temperatures. Upon photolysis at 10 K, ACH retains significantly larger fractions of photoproducts, primarily CO and CH_3CH_2OH, whereas pure and mixed ices favor CO and CH_4 formation. Furthermore, upon warming to 130 K, UV-photolyzed ACH seeded new CHs of CO and CO_2, an outcome absent in the photolyzed acetaldehyde + H_2O sample. These findings demonstrate that clathrate cages not only modulate photochemical reaction pathways but also enhance product trapping, highlighting their potential role in the chemical evolution of astrophysical ices.

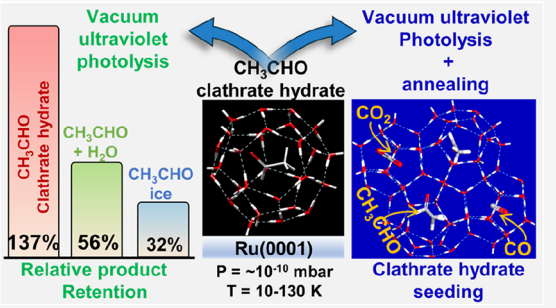

Clathrate hydrates (CHs) are nonstoichiometric crystalline structures in which water molecules form cages that encapsulate guest species.[1] Found in high-pressure, low-temperature terrestrial environments, such as ocean sediments and permafrost, CHs are widely studied for carbon storage and energy applications involving gases such as CO_2, CH_4, and H_2.[2−9] Recently, CHs have attracted attention in astrochemistry, as observations suggest their presence on icy bodies in the outer solar system and potentially in the interstellar environments.[10−17] Their ability to trap volatile organic molecules makes them potential reservoirs of complex organics in space.[18] However, experimental studies on the effects of interstellar radiation (e.g., electrons, protons, and UV), on CHs remain limited.

UV photolysis of molecular solids generates radicals and reactive intermediates that can recombine, diffuse, or desorb, leading to secondary products. In CHs, the cage structure may stabilize reactive species and influence reaction pathways and product retention.[18] We have previously demonstrated the formation of CHs with various guest molecules,[12,19−25] including acetaldehyde (CH_3CHO),[13] under ultrahigh vacuum (UHV, $\sim 10^{-10}$ mbar) and cryogenic temperatures (10−130 K) using techniques such as reflection absorption infrared spectroscopy (RAIRS), temperature-programmed desorption mass spectrometry (TPD-MS), and, more recently, electron diffraction.[26] These studies establish the stability of CHs under astrophysically relevant conditions and motivate investigation of their photochemical behavior. Key questions remain: How CHs respond to UV irradiation, whether they alter reaction pathways relative to pure or mixed ices, and how confinement affects product selectivity and retention. Addressing these questions is critical as CHs may exhibit behavior markedly different from conventional amorphous or crystalline ice matrices in terms of guest retention and release.[10]

Acetaldehyde, detected in molecular clouds, star-forming regions, and comets, is a key precursor to prebiotic molecules such as sugars and amino acids.[27−29] Despite its lower interstellar abundance (~1−10% relative to water), it has been widely studied experimentally under various radiations to comprehend its role in forming complex organics.[29,30] Studying the photochemical and subsequent thermal processing of ACH may provide insight into the role of CHs as molecular reservoirs and potential seeds for new CHs under UHV conditions.

Gamma-ray irradiation of CHs formed at high pressures has been shown to induce hydrogen-transfer reactions between confined radicals and guest molecules.[33−35] Our previous work extended this to UV irradiation,[36] showing that CO_2 CH

Received: March 19, 2026
Revised: April 22, 2026
Accepted: May 5, 2026

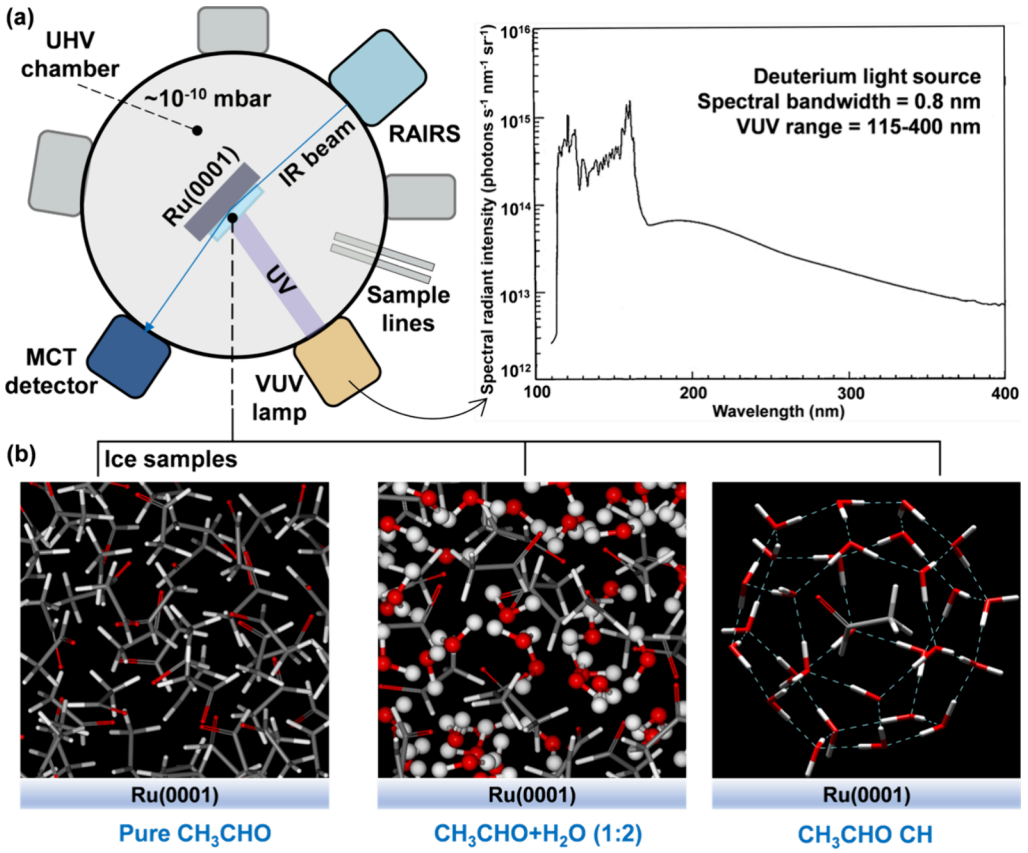

Figure 1. (a) Schematic of the UHV apparatus demonstrating the key components, including the metal substrate, VUV lamp (with emission spectra), RAIRS, MCT detector, and sample lines. Only the tools relevant to this study are displayed for clarity. A thorough description can be found in our previous work.[21,31,32] (b) Schematic of the initial composition of the ices: pure acetaldehyde, acetaldehyde + H_2O (1:2) mixed ice, and ACH, at 10 K. H_2O molecules are represented using distinct styles (ball-and-stick or stick) for clear differentiation across samples. Color code: carbon (gray), oxygen (red), and hydrogen (white). Hydrogen bonding is shown as dotted lines in cyan.

release trapped CO_2 to the amorphous ice matrix without forming new photoproducts, whereas dimethyl ether CH exhibits cage-mediated chemistry, suggesting that CHs can act as nanoreactors.[37] Building on this, here, we investigate UV photolysis of pure acetaldehyde, acetaldehyde + H_2O mixed ice, and acetaldehyde clathrate hydrate (ACH) under interstellar-like conditions (~10^{-10} mbar, 10 K) using RAIRS. Further, the photolyzed samples at 10 K, containing simple and complex molecules were annealed to 130 K to examine their physicochemical properties, in view of their similarity to cometary and interstellar ices.

To begin with, we photolyzed pure acetaldehyde, acetaldehyde + H_2O (1:2) mixed ice, and ACH (Figure 1a,b) for 1 h at 10 K under UHV, monitoring the resulting changes using RAIRS. Additional experimental details are given in the Supporting Information. Figure 1b provides a schematic of the ice compositions prior to photolysis, with corresponding full-range RAIR spectra shown in Figure S1. VUV exposure of these samples produced multiple photoproducts, as detected by RAIRS and shown in Figures 2a-c. Across all samples, common photoproducts detected are CO (2136 cm^{-1}),[38,39] CO_2 (~2340 cm^{-1}),[38,39] CH_4 (1304 cm^{-1}),[39,40] HOCO (1261 cm^{-1}),[41,42] CH_3OCH_3 (1150 cm^{-1}),[43,44] $HOCH_2CH_2OH$ (1088 cm^{-1}),[44,45] and CH_3CH_2OH (1050 cm^{-1}).[39,43] However, pure acetaldehyde uniquely yielded ketene (H_2CCO, 2129 cm^{-1})[46,47] and hydroxymethyl radical (CH_2OH, 1194 cm^{-1}).[45,48] CH_3CH_2OH was present in all samples, while CH_3OH (1017 cm^{-1})[39,49] was specific to the samples with H_2O, with its highest production observed in the acetaldehyde + H_2O mixed ice. Tables S1 and S2 list band assignments for reactants and photoproducts, with peak positions consistent with previous studies, confirming spectral data reliability. Figure S2a compares photoproducts from the photolysis of pure acetaldehyde, acetaldehyde + H_2O (1:2) mixed ice, and ACH at 10 K, while Figure S2b outlines a plausible formation pathway for these photoproducts. Notably, the IR peak position of ketene overlaps with that of CO (Figure 2a). Therefore, ketene formation was further confirmed by annealing the photolyzed pure acetaldehyde sample to ~100 K, at which point CO desorbed while ketene remained, as illustrated in Figure S3. Similar confirmation methods have been employed in previous studies.[46,47]

We quantified the photodissociation of acetaldehyde and subsequent photoproduct formation across the samples, as depicted in Figures 3a-d. To account for varying initial acetaldehyde concentrations, we normalized the column densities of all photoproducts relative to each sample's initial acetaldehyde concentration (more details are provided in the Supporting Information). Figure 3a shows acetaldehyde photodissociation, while Figures 3b-d illustrate changes in normalized column densities of major photoproducts (CH_4, CO_2, CO, H_2CCO, CH_3OH, CH_3CH_2OH) produced in pure acetaldehyde, acetaldehyde + H_2O (1:2) mixed ice, and ACH at 10 K during 0−60 min of VUV photolysis. The relative extent of photodissociation of acetaldehyde across the samples follows the order pure acetaldehyde > acetaldehyde + H_2O

https://doi.org/10.1021/acs.jpclett.6c00885
J. Phys. Chem. Lett. XXXX, XXX, XXX−XXX

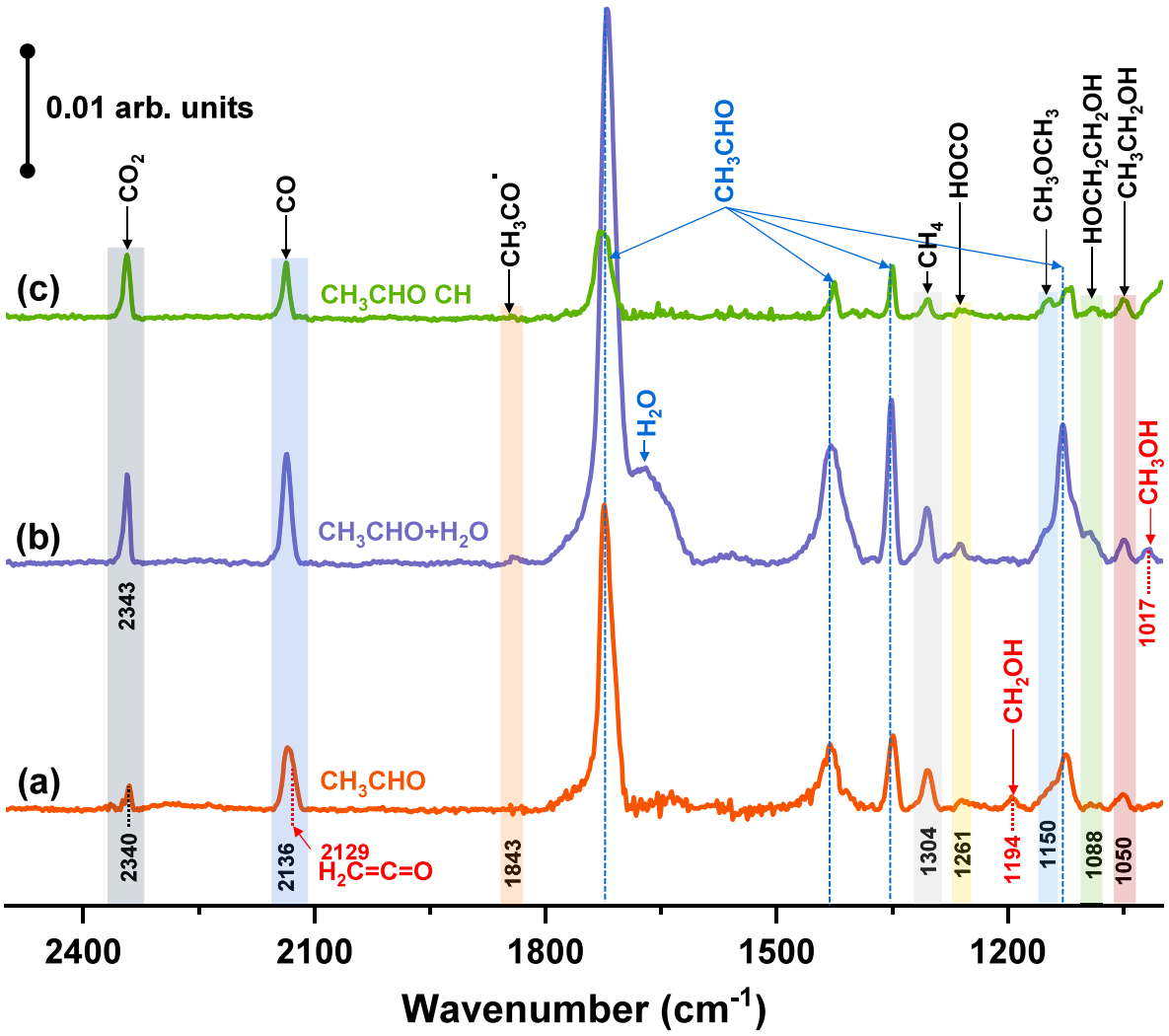

Figure 2. RAIR spectra (2500−1000 cm^{-1}) showing the changes after 1 h of VUV photolysis at 10 K of (a) ∼100 ML pure acetaldehyde ice, (b) ∼300 ML acetaldehyde + H_2O (1:2) mixed ice, and (c) ACH. The ACH sample was prepared by annealing ∼300 ML acetaldehyde + H_2O (1:2) mixed ice from 10 to 137 K.[13] Then it was cooled back to 10 K for photolysis. Key IR bands corresponding to the formed photoproducts are highlighted and marked. Red-marked photoproducts are unique to the sample and absent in other samples. Major IR bands corresponding to the reactant acetaldehyde are marked by vertical dashed lines.

mixed ice > ACH (Figure 3a). The dominant photoproducts were CH_4 followed by CO in the pure acetaldehyde sample (Figure 3b), CO followed by CH_4 in the acetaldehyde + H_2O mixed ice (Figure 3c), and CO followed by CH_3CH_2OH in ACH (Figure 3d). These results suggest that ACH provides a distinct chemical environment for the photolysis of acetaldehyde, favoring the formation of CH_3CH_2OH over other photoproducts. Scheme 1 illustrates the decomposition order of acetaldehyde across different samples and the relative abundances of its top three photoproducts.

Moreover, to demonstrate photoproduct retention trends following 1 h of VUV photolysis at 10 K, we compared the cumulative normalized column densities of key photoproducts (CH_4, CO, CO_2, CH_3CH_2OH) across the three samples (Figure 4a). Calculation details are provided in the Supporting Information. In the pure acetaldehyde sample, only 32.38% of these photoproducts were retained during photolysis, comprising 14.96% CH_4, 0.49% CO_2, 9.95% CO, and 6.98% CH_3CH_2OH. The acetaldehyde + H_2O mixed ice retained about 56.17% relative to the total photodissociated acetaldehyde. Remarkably, ACH showed a retention of approximately 136.95%, suggesting that CHs serve as molecular reservoirs, retaining photoproducts more effectively than amorphous or mixed systems during photolysis at 10 K. To the best of our knowledge, this is the first experimental demonstration of CHs acting as molecular reservoirs under such conditions.

The retention of photoproducts by 136.95% in the ACH sample can be explained by two factors: (i) a single unit of acetaldehyde (along with H_2O) produces multiple units of photoproducts (Figure S2b), and (ii) CH cages can trap radicals and reactive volatile species more efficiently than pure and mixed acetaldehyde ices, facilitating further reactions. In the case of ACH, 31.74% of the photoproducts were CH_4, 8.74% were CO_2, 55.91% were CO, and 40.56% were CH_3CH_2OH. This indicates that ∼40% of the total photodissociated acetaldehyde was converted into CH_3CH_2OH, as the formation of one unit of CH_3CH_2OH requires one unit of acetaldehyde ($CH_3CHO + 2H \rightarrow CH_3CH_2OH$).[50,51] It is worth noting that production of CH_3CH_2OH was about 7 and 9% in pure and mixed acetaldehyde ices, respectively (Figure 4a).

https://doi.org/10.1021/acs.jpclett.6c00885
J. Phys. Chem. Lett. XXXX, XXX, XXX−XXX

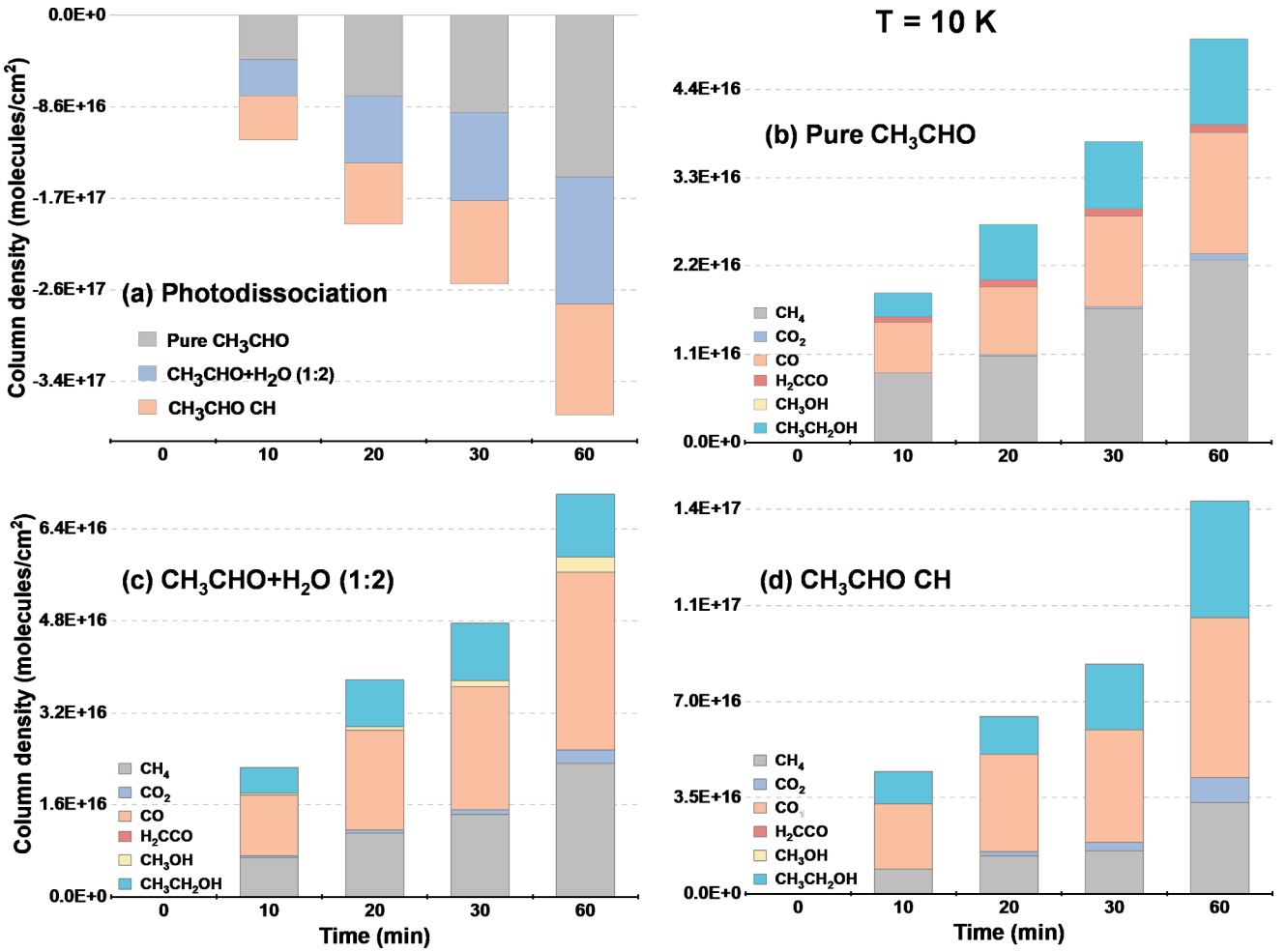

Figure 3. (a) Variation in normalized column densities of acetaldehyde during photodissociation of pure acetaldehyde ice, acetaldehyde + H_2O (1:2) mixed ice, and ACH as a function of VUV irradiation time. Similarly, (b, c, and d) depict the changes in normalized column densities of various photoproducts (CH_4, CO_2, CO, H_2CCO, CH_3OH, CH_3CH_2OH) with VUV photolysis time, resulting from the photolysis of pure acetaldehyde ice, acetaldehyde + H_2O (1:2) mixed ice, and ACH at 10 K, respectively.

Scheme 1. Trends of VUV-Induced Decomposition of Acetaldehyde in Different Ice Matrices and Their Major Photoproducts

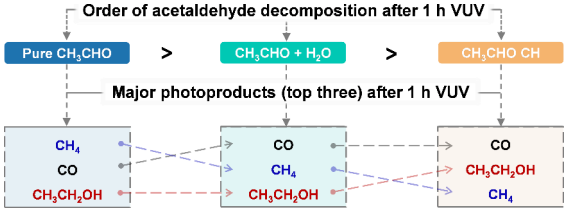

Although the formation of CH_3CH_2OH from CH_3CHO can be formally represented as addition of two H atoms, the underlying mechanism is likely more complex under cryogenic conditions. CH_3CH_2OH formation may proceed via indirect pathways involving intermediates such as H_2CCO and vinyl alcohol (CH_2CHOH).[52,53] In the present study, H_2CCO was detected, whereas CH_2CHOH was not directly observed, although matrix-isolation studies have shown that acetaldehyde can form CH_2CHOH as a primary product under radiation-induced conditions.[54] The absence of a clear CH_2CHOH signature in our spectra is likely due to overlap of its characteristic band (1077−1082 cm^{-1})[54] with a band at ∼1088 cm^{-1} assigned to $HOCH_2CH_2OH$, and therefore its transient formation cannot be excluded. In addition, along direct pathways, reaction of H atoms with CH_3CHO can proceed via competing abstraction and addition channels, and the branching between these pathways may depend on the local environment, including confinement within hydrate cages.[55,56] If addition occurs, intermediate radical species such as α-hydroxyethyl (CH_3CHOH) and/or CH_3CH_2O would be expected.[55] However, no unambiguous spectroscopic signatures of these intermediates were identified. In particular, the CH_3CHOH band[55] reported near 1048−1050 cm^{-1} overlaps with the CH_3CH_2OH band (∼1050 cm^{-1}), preventing definitive assignment. Thus, these observations suggest that CH_3CH_2OH formation may proceed via multiple competing pathways, including direct hydrogenation and indirect routes involving CH_2CHOH and H_2CCO intermediates. However, the absence of clear intermediate signatures precludes definitive identification of the dominant mechanism under the present conditions.

The production of CH_3CH_2OH from acetaldehyde-containing ices during energetic processing has been challenging to observe.[29,51] However, both observational and theoretical evidence indicate that alcohols (e.g., CH_3CH_2OH) can form through the hydrogenation of aldehydes (e.g., CH_3CHO),

https://doi.org/10.1021/acs.jpclett.6c00885
J. Phys. Chem. Lett. XXXX, XXX, XXX−XXX

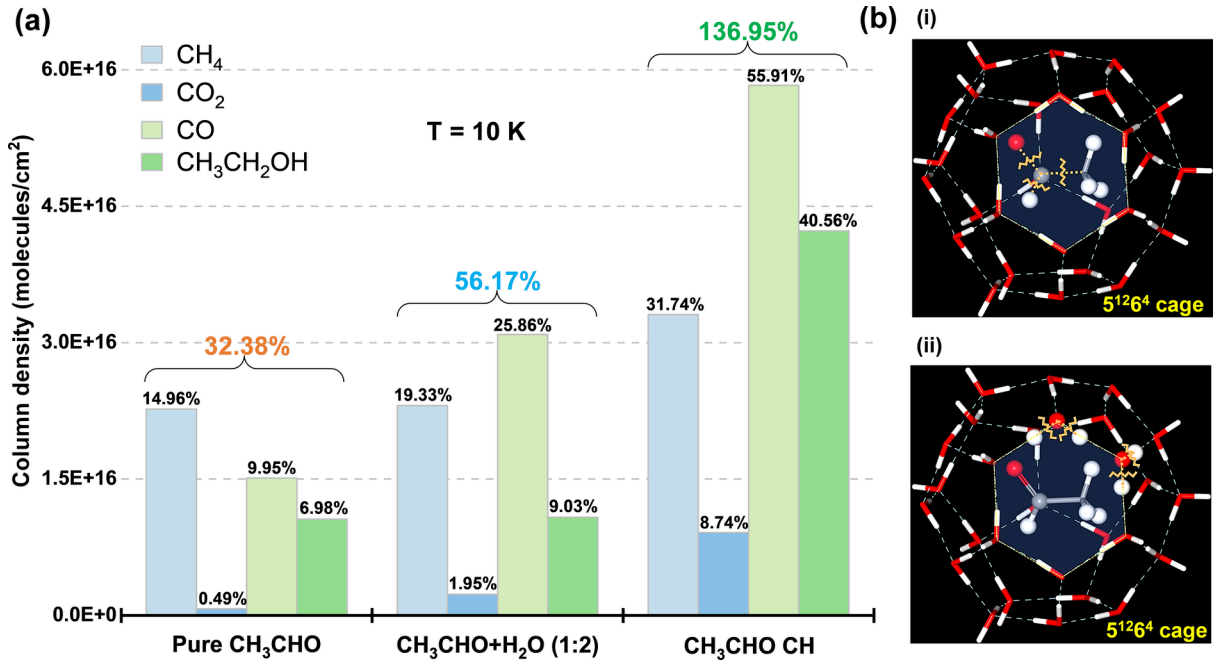

Figure 4. (a) Comparison of the retention of key photoproducts (e.g., CH_4, CO_2, CO, CH_3CH_2OH) identified through RAIRS analysis following 1 h of VUV photolysis of pure acetaldehyde, acetaldehyde + H_2O (1:2) mixed ice, and ACH at 10 K. Here, the photoproducts are expressed as a percentage (%) of the total photodissociated acetaldehyde during photolysis, with the cumulative percentage of these major photoproducts for each sample displayed at the top of the columns. (b) Schematic representation of VUV photolysis scenarios in the ACH sample: (i) photodissociation of acetaldehyde molecules inside the $5^{12}6^4$ CH cages and (ii) photolysis of H_2O molecules forming the $5^{12}6^4$ cages. A blue, partially transparent hexagonal shape with a yellow outline is used in (i) and (ii) to symbolize a hexagonal plane of $5^{12}6^4$ cages.

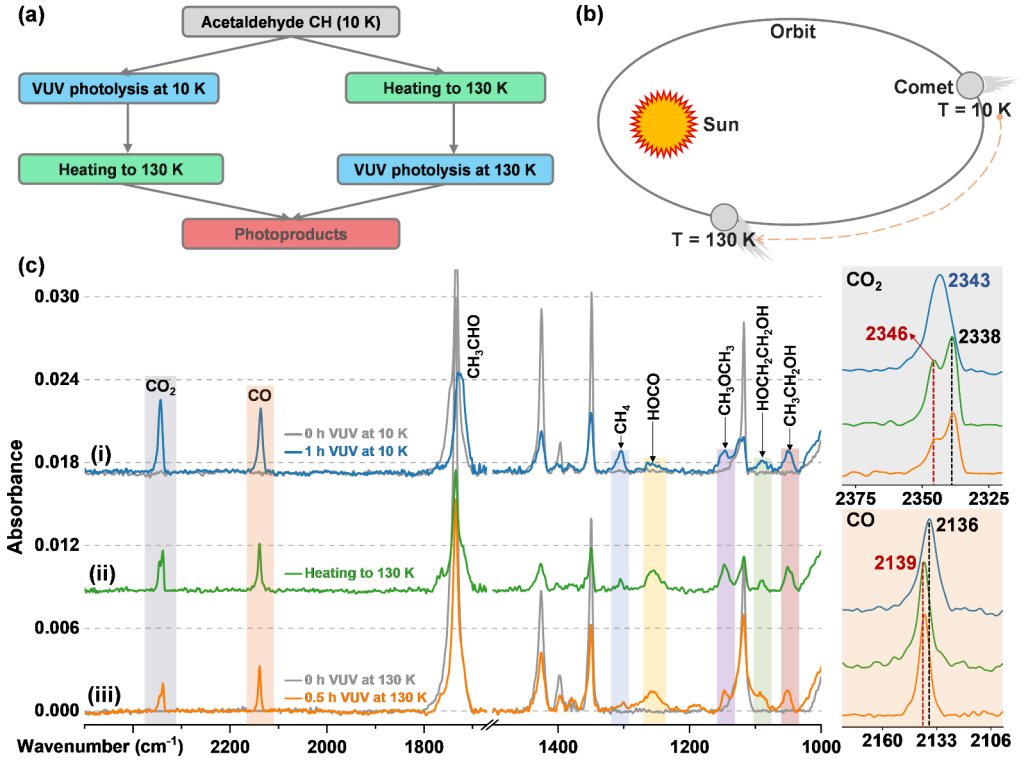

Figure 5. (a) Schematic overview of the experimental procedure for the photolysis of ACH at 10 and 130 K. (b) Illustration of a comet's orbit around the sun, highlighting the temperature rise as the comet approaches the sun. (c) RAIR spectra showing the changes (i) before and after photolysis of ACH at 10 K, (ii) after annealing the photolyzed ACH sample from 10 to 130 K, and (iii) before and after photolysis of ACH at 130 K. Insets provide a zoomed in view of changes in the CO_2 and CO bands highlighted by light gray and light orange shades, respectively.

ketones, and ketenes under similar conditions.[52,53] In the current work, substantial CH_3CH_2OH production in ACH can be attributed to the unique chemical environment provided by the CH structure, where cages act as "tiny reaction vessels"

https://doi.org/10.1021/acs.jpclett.6c00885
J. Phys. Chem. Lett. XXXX, XXX, XXX−XXX

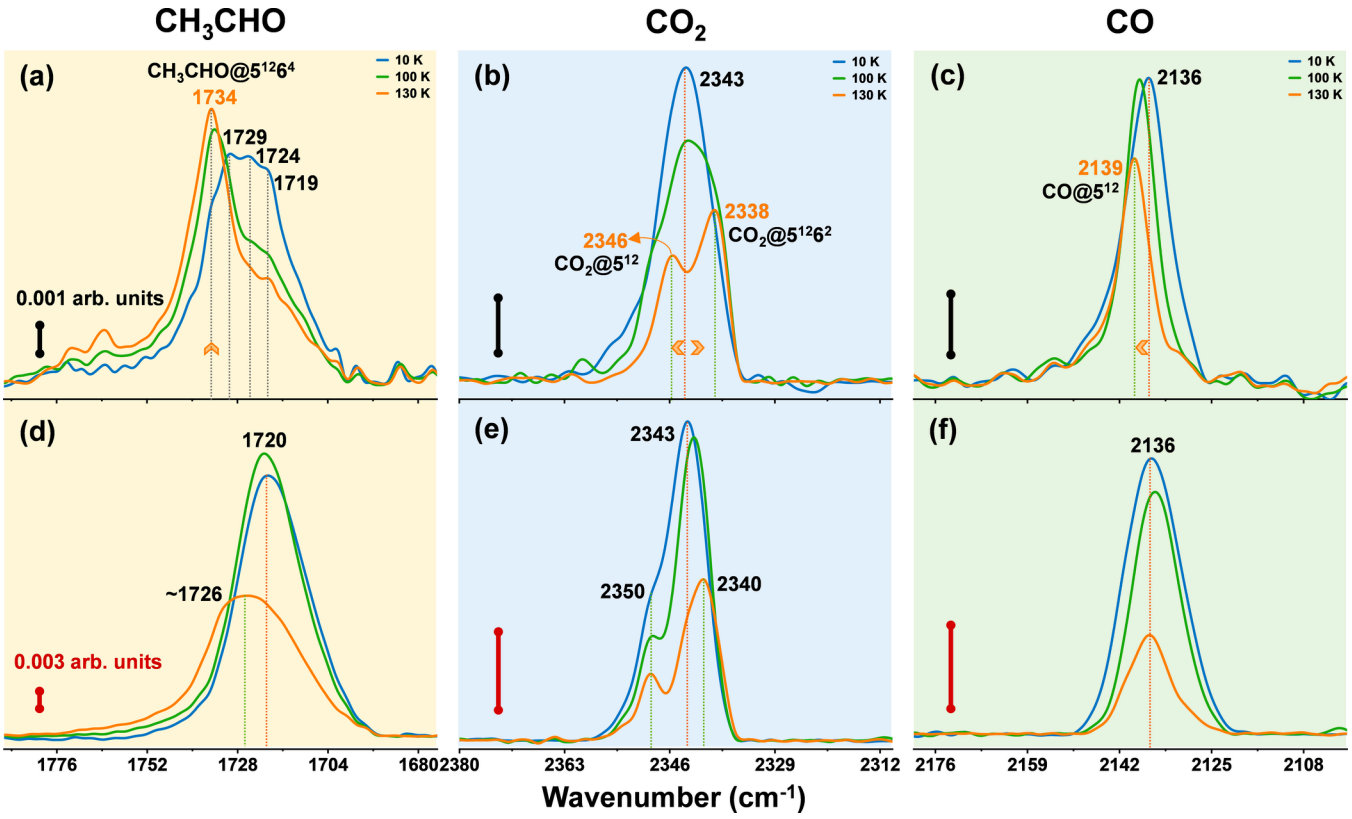

Figure 6. Temperature-dependent RAIR spectra of VUV-photolyzed samples (1 h of VUV at 10 K), annealed from 10 K to 130 K at a rate of 5 K/min: (a-c) ACH sample and (d-f) acetaldehyde + H_2O (1:2) mixed ice. Panels show spectra for the (a, d) C═O stretching region of acetaldehyde, (b, e) C═O antisymmetric stretching region of CO_2, and (c, f) C═O stretching region of CO. The black and red vertical lines in the top and bottom panels represent absorbance scales of 0.001 and 0.003, respectively.

facilitating distinct chemical synthesis. During VUV photolysis of ACH, acetaldehyde breakdown can proceed via three pathways: (1) photolysis inside clathrate cages with radicals reacting among themselves or with H_2O molecules (Figure 4b(i)); (2) photodissociation of H_2O molecules of the clathrate cages, with photoproducts reacting with acetaldehyde (Figure 4b(ii)); or (3) simultaneous photodissociation of both H_2O and acetaldehyde inside the cages, leading to secondary photoproducts. CH, thus, provides a unique environment for chemical synthesis and efficiently retain photoproducts during VUV photolysis compared to pure or mixed amorphous ices.

Furthermore, to assess the temperature-dependent effects of VUV light on CHs, we photolyzed ACH at 10 and 130 K, simulating conditions experienced by comets and icy bodies, as illustrated in Figures 5a-c. Figure 5c shows the RAIR spectra for the (i) VUV photolysis of ACH at 10 K, (ii) subsequent annealing of the photolyzed sample to 130 K, and (iii) direct photolysis of ACH at 130 K. The photoproducts detected at both the temperatures were similar; however, their distribution differed. At 10 K, simple molecules such as CO, CO_2, and CH_4 were more abundant, whereas at 130 K, complex molecules like CH_3OCH_3, $HOCH_2CH_2OH$, and CH_3CH_2OH dominated. This shift likely results from the enhanced desorption of simple species at 130 K, reducing their retention, while at 10 K, limited diffusion of radicals suppresses the formation of complex products. The inset in Figure 5c compares the RAIR spectra of CO and CO_2. It reveals that the spectra are identical for the sample photolyzed at 10 K and then warmed to 130 K, and the sample directly photolyzed at 130 K. However, larger fraction of photoproducts was retained in the sample that was photolyzed at 10 K before annealing.

Recent observations from the James Webb Space Telescope (JWST) have identified complex organic molecules in interstellar ices, such as CH_3CHO, CH_3CH_2OH, methyl formate (CH_3OCHO), and formic acid (CH_3COOH), alongside previously known simple molecules like H_2O, CO, CO_2, CH_4, CH_3OH, and ammonia (NH_3).[57] In our study, VUV photolysis of ACH and acetaldehyde + H_2O mixed ices at 10 K produced ices containing both simple (H_2O, CO, CO_2, CH_4, CH_3OH) and complex molecules (CH_3OCH_3, $HOCH_2CH_2OH$, CH_3CH_2OH, etc.) with or without ACH. Such composite ice samples are challenging to create experimentally at 10 K without photolysis, making our postphotolysis samples closely resemble those found on comets and icy satellites. Following photolysis, we performed thermal processing on these composite ice samples by heating them from 10 to 130 K and monitoring the changes using RAIRS, as illustrated in Figure 6. This represents the first thermal processing of composite ice samples containing CHs, simple molecules, and complex organics under UHV and cryogenic conditions.

Figure 6 presents the RAIR spectra showing evolution of acetaldehyde, CO_2, and CO within composite ices formed through the photolysis of the ACH sample (top panels: a-c) and acetaldehyde + H_2O mixed ice (bottom panels: d-f) in their respective C═O stretching regions over the 10−130 K temperature range. In Figure 6a, the RAIR spectrum at 10 K (blue trace) exhibits peaks at 1719, 1724, 1729, and 1734 cm^{-1}, where the 1719 and 1729 cm^{-1} peaks correspond

https://doi.org/10.1021/acs.jpclett.6c00885
J. Phys. Chem. Lett. XXXX, XXX, XXX−XXX

to acetaldehyde in a water matrix, 1734 cm^{-1} is attributed to ACH, and 1724 cm^{-1} is likely attributed to production of formaldehyde.[13,58] As the composite ice sample, containing a small fraction of ACH along with various simple and complex molecules, was annealed from 10 to 130 K, the peak at 1734 cm^{-1} increased while the others diminished, indicating the conversion of free acetaldehyde in the water matrix to ACH and partial desorption.[13] Similarly, in the C═O antisymmetric stretching region of CO_2 (Figure 6b), the spectrum at 10 K shows a peak at 2343 cm^{-1}, corresponding to CO_2 in a water-dominated ice matrix.[21,59] Upon annealing to 130 K, this peak splits into two at 2346 and 2338 cm^{-1}, which are assigned to CO_2 trapped in the small 5^{12} and large $5^{12}6^2$ cages of the CHs, respectively.[60,61] Given the presence of other hydrate-forming molecules such as acetaldehyde and methanol in the ice matrix, CO_2 may form a mixture of structure I (sI) CH (occupying 5^{12} and $5^{12}6^2$ cages) and structure II (sII) CH (with CO_2 in 5^{12} cages and larger molecules in $5^{12}6^4$ cages). Notably, the formation of CO_2 CH during the annealing of H_2O–CO_2 ices at ∼120 K has been reported previously.[21,62] Figure 6c illustrates the evolution of CO in the C═O stretching region. The broad peak at 2136 cm^{-1} at 10 K was shifted to 2139 cm^{-1}, became sharper, and slightly decreased in intensity as the sample was heated to 130 K. Pure CO is known to desorb from ice matrices below 50 K;[32] however, the retention of CO at 130 K indicates its trapping within CH cages. Thus, the peak at 2139 cm^{-1} at 130 K is attributed to CO occupying the small 5^{12} cages of CHs which may belong to either sI or sII (as discussed above).

In the photolyzed acetaldehyde + H_2O mixed ice (Figure 6d), the 1720 cm^{-1} peak associated with acetaldehyde at 10 K decreased in intensity and got broadened upon annealing to 130 K. Notably, the 1734 cm^{-1} peak, indicative of ACH, did not appear, confirming its absence in the composite ice. It is worth mentioning that our previous study demonstrated that acetaldehyde in mixed acetaldehyde + H_2O ices can form CH at 115 K under UHV conditions.[13]

For CO_2 (Figure 6e), the 2343 cm^{-1} peak at 10 K was split into peaks at 2350 and 2340 cm^{-1} upon annealing, attributed to CO_2 trapped in amorphous solid water matrix, which further confirms the absence of CO_2 CH. In the case of CO (Figure 6f), the 2136 cm^{-1} peak observed at 10 K remained unchanged in position but significantly decreased in intensity upon annealing to 130 K, indicating CO desorption from the composite ice matrix. This is likely due to the absence of clathrate cages to retain CO. A comparison of the areas under the curves for Figures 6c and 6f, plotted as a function of temperature (10–130 K) in Figure S4, demonstrated greater CO desorption in the photolyzed acetaldehyde + H_2O mixed ice than in photolyzed ACH composite ice. The findings indicate that annealing the composite ice, formed after ACH photolysis (containing a small fraction of ACH, free acetaldehyde, as well as simple and complex molecules) from 10 to 130 K, not only promotes reformation of more ACH but also facilitates the formation of new CHs of CO_2 and CO within the composite ice matrix.

These results demonstrate that CHs can significantly influence the photochemistry of cometary and interstellar ices by trapping volatile molecules and creating environments conducive to complex organic synthesis. However, the nature of this energetic processing depends strongly on the radiation profile. In this work, VUV radiation was provided by a deuterium lamp with a broad emission spectrum (115–400 nm; ∼3.1–10.8 eV). This energy range can induce a range of electronic transitions in acetaldehyde, including valence ($n \rightarrow \pi^*$, $\pi \rightarrow \pi^*$) and higher-lying Rydberg states, while also approaching the molecule's ionization threshold (∼10.2 eV).[63] While this broadband irradiation enables a broad survey of photochemical reactivity, it simultaneously populates multiple excited states, making it difficult to assign specific reaction pathways. In contrast, state-specific monochromatic irradiation (e.g., 193 or 185 nm) would allow selective excitation of individual electronic states. Such an approach would be valuable in future studies to disentangle competing pathways and better understand the underlying photochemical mechanisms. Moving toward such state-resolved investigations will be important for developing a more detailed understanding of molecular evolution in astrophysical ice environments.

In conclusion, by photolyzing and subsequently thermally processing pure acetaldehyde, acetaldehyde + H_2O mixed ice, and ACH under UHV and cryogenic temperatures, we found that CHs not only preserve volatile molecules but also act as "tiny reaction vessels" providing unique environments for chemical transformations. While CHs of simple molecules (such as CH_4 and C_2H_6) have been detected in astrophysical environments,[10] our study suggests that their formation may be initiated by CHs of more complex molecules, such as acetaldehyde. These findings advance our understanding of CH-mediated organic transformations and the potential for preserving prebiotic molecules on icy bodies across the solar system and beyond. Future research will explore the photochemical and thermal processing of several other CHs to elucidate their impact on the chemical evolution of interstellar and cometary ices through both experimental and computational approaches.

■ ASSOCIATED CONTENT

Supporting Information

The Supporting Information is available free of charge at https://pubs.acs.org/doi/10.1021/acs.jpclett.6c00885.

Experimental section, full-range RAIR spectra of acetaldehyde ices before photolysis, list of characteristic IR bands of reactants and photoproducts with spectral assignments, proposed formation pathways for various photoproducts identified via RAIRS analysis, temperature-dependent RAIR spectra of VUV-photolyzed pure acetaldehyde ice, and integrated area of the C═O stretching band plotted against temperature (PDF)

■ AUTHOR INFORMATION

Corresponding Authors

Rajnish Kumar − *Department of Chemical Engineering, Indian Institute of Technology Madras, Chennai 600036, India; International Centre for Clean Water, IIT Madras Research Park, Chennai 600113, India;* orcid.org/0000-0002-4172-2638; Email: rajnish@iitm.ac.in

Thalappil Pradeep − *DST Unit of Nanoscience (DST UNS) and Thematic Unit of Excellence (TUE), Department of Chemistry, Indian Institute of Technology Madras, Chennai 600036, India; International Centre for Clean Water, IIT Madras Research Park, Chennai 600113, India;* orcid.org/0000-0003-3174-534X; Email: pradeep@iitm.ac.in

https://doi.org/10.1021/acs.jpclett.6c00885
J. Phys. Chem. Lett. XXXX, XXX, XXX−XXX

Authors

Gaurav Vishwakarma − *DST Unit of Nanoscience (DST UNS) and Thematic Unit of Excellence (TUE), Department of Chemistry, Indian Institute of Technology Madras, Chennai 600036, India;* Present Address: Department of Chemical and Biomolecular Engineering, National University of Singapore, Singapore 117580, Singapore; orcid.org/0009-0002-6076-3299

Soham Chowdhury − *DST Unit of Nanoscience (DST UNS) and Thematic Unit of Excellence (TUE), Department of Chemistry, Indian Institute of Technology Madras, Chennai 600036, India;* orcid.org/0009-0000-8151-6065

Complete contact information is available at: https://pubs.acs.org/10.1021/acs.jpclett.6c00885

Author Contributions

G.V. designed the experiments and, together with S.C., performed the experimental work. The progress of the study was supervised and validated by T.P. and R.K. G.V. analyzed the experimental data and prepared the initial draft of the manuscript. The final version of the manuscript was completed with contributions and revisions from all authors.

Notes

The authors declare no competing financial interest.

■ ACKNOWLEDGMENTS

T.P. acknowledges funding from the Science and Engineering Research Board (SERB), Department of Science and Technology (DST), Government of India for research funding. T.P. and R.K. acknowledge funding from the Centre of Excellence on Molecular Materials and Functions under the Institution of Eminence scheme of IIT Madras. G.V. and S.C. thank IITM for their research fellowships.

■ REFERENCES

(1) Sloan, E. D. Fundamental Principles and Applications of Natural Gas Hydrates. *Nature* **2003**, *426*, 353−359.

(2) Boswell, R. Is Gas Hydrate Energy within Reach? *Science (80-.).* **2009**, *325* (5943), 957−958.

(3) Park, Y.; Kim, D. Y.; Lee, J. W.; Huh, D. G.; Park, K. P.; Lee, J.; Lee, H. Sequestering Carbon Dioxide into Complex Structures of Naturally Occurring Gas Hydrates. *Proc. Natl. Acad. Sci. U.S.A.* **2006**, *103* (34), 12690−12694.

(4) Bhattacharjee, G.; Goh, M. N.; Arumuganainar, S. E. K.; Zhang, Y.; Linga, P. Ultra-Rapid Uptake and the Highly Stable Storage of Methane as Combustible Ice. *Energy Environ. Sci.* **2020**, *13* (12), 4946−4961.

(5) Babu, P.; Linga, P.; Kumar, R.; Englezos, P. A Review of the Hydrate Based Gas Separation (HBGS) Process Forcarbon Dioxide Pre-Combustion Capture. *Energy* **2015**, *85*, 261−279.

(6) Veluswamy, H. P.; Kumar, R.; Linga, P. Hydrogen Storage in Clathrate Hydrates: Current State of the Art and Future Directions. *Appl. Energy* **2014**, *122*, 112−132.

(7) Vishwakarma, G.; Dhamu, V.; Qureshi, M. F.; Bhattacharjee, G.; Pradeep, T.; Linga, P. Understanding the Kinetics of CO2 Hydrate Formation in Dry Water for Carbon Capture and Storage: X-Ray Diffraction and In Situ Raman Studies. *ACS Appl. Mater. Interfaces* **2025**, *17* (3), 4865−4874.

(8) Zhang, Y.; Ma, Y.; Jeenmuang, K.; Vishwakarma, G.; Sun, C.-Y.; Chen, G.-J.; Linga, P. Rapid Conversion of Amino Acid Modified-Ice to Methane Hydrate for Sustainable Energy Storage. *Nat. Commun.* **2025**, *16* (1), 8670.

(9) Vishwakarma, G.; Hondo, E.; Jeenmuang, K.; Kumar, R.; Linga, P. Isoxazole-Stabilized Clathrate Hydrate for Hydrogen Storage. *J. Phys. Chem. Lett.* **2026**, *17* (7), 2145−2151.

(10) Luspay-Kuti, A.; Mousis, O.; Hässig, M.; Fuselier, S. A.; Lunine, J. I.; Marty, B.; Mandt, K. E.; Wurz, P.; Rubin, M. The Presence of Clathrates in Comet 67P/Churyumov-Gerasimenko. *Sci. Adv.* **2016**, *2* (4), e1501781−e1501781.

(11) Tobie, G.; Lunine, J. I.; Sotin, C. Episodic Outgassing as the Origin of Atmospheric Methane on Titan. *Nature* **2006**, *440* (7080), 61−64.

(12) Ghosh, J.; Methikkalam, R. R. J.; Bhuin, R. G.; Ragupathy, G.; Choudhary, N.; Kumar, R.; Pradeep, T. Clathrate Hydrates in Interstellar Environment. *Proc. Natl. Acad. Sci. U.S.A.* **2019**, *116* (5), 1526−1531.

(13) Vishwakarma, G.; Malla, B. K.; Chowdhury, S.; Khandare, S. P.; Pradeep, T. Existence of Acetaldehyde Clathrate Hydrate and Its Dissociation Leading to Cubic Ice under Ultrahigh Vacuum and Cryogenic Conditions. *J. Phys. Chem. Lett.* **2023**, *14* (23), 5328−5334.

(14) Mousis, O.; Lunine, J. I.; Picaud, S.; Cordier, D. Volatile Inventories in Clathrate Hydrates Formed in the Primordial Nebula. *Faraday Discuss.* **2010**, *147*, 509−525.

(15) Thomas, C.; Mousis, O.; Picaud, S.; Ballenegger, V. Variability of the Methane Trapping in Martian Subsurface Clathrate Hydrates. *Planet. Space Sci.* **2009**, *57* (1), 42−47.

(16) Swindle, T. D.; Thomas, C.; Mousis, O.; Lunine, J. I.; Picaud, S. Incorporation of Argon, Krypton and Xenon into Clathrates on Mars. *Icarus* **2009**, *203* (1), 66−70.

(17) Ghosh, J.; Vishwakarma, G.; Kumar, R.; Pradeep, T. Formation and Transformation of Clathrate Hydrates under Interstellar Conditions. *Acc. Chem. Res.* **2023**, *56* (16), 2241−2252.

(18) Goldberg, P. Free Radicals and Reactive Molecules in Clathrate Cavities. *Science (80-.).* **1963**, *142* (3590), 378−379.

(19) Ghosh, J.; Bhuin, R. G.; Vishwakarma, G.; Pradeep, T. Formation of Cubic Ice via Clathrate Hydrate, Prepared in Ultrahigh Vacuum under Cryogenic Conditions. *J. Phys. Chem. Lett.* **2020**, *11* (1), 26−32.

(20) Ghosh, J.; Vishwakarma, G.; Das, S.; Pradeep, T. Facile Crystallization of Ice I_h via Formaldehyde Hydrate in Ultrahigh Vacuum under Cryogenic Conditions. *J. Phys. Chem. C* **2021**, *125* (8), 4532−4539.

(21) Vishwakarma, G.; Malla, B. K.; Reddy, K. S. S. V. P.; Ghosh, J.; Chowdhury, S.; Yamijala, S. S. R. K. C.; Reddy, S. K.; Kumar, R.; Pradeep, T. Induced Migration of CO2 from Hydrate Cages to Amorphous Solid Water under Ultrahigh Vacuum and Cryogenic Conditions. *J. Phys. Chem. Lett.* **2023**, *14*, 2823−2829.

(22) Malla, B. K.; Vishwakarma, G.; Chowdhury, S.; Selvarajan, P.; Pradeep, T. Formation of Ethane Clathrate Hydrate in Ultrahigh Vacuum by Thermal Annealing. *J. Phys. Chem. C* **2022**, *126* (42), 17983−17989.

(23) Ghosh, J.; Bhuin, R. G.; Ragupathy, G.; Pradeep, T. Spontaneous Formation of Tetrahydrofuran Hydrate in Ultrahigh Vacuum. *J. Phys. Chem. C* **2019**, *123*, 16300−16307.

(24) Malla, B. K.; Vishwakarma, G.; Chowdhury, S.; Nayak, S. K.; Yamijala, S. S. R. K. C.; Pradeep, T. Formation and Dissociation of Dimethyl Ether Clathrate Hydrate in Interstellar Ice Mimics. *J. Phys. Chem. C* **2024**, *128* (6), 2463−2470.

(25) Chowdhury, S.; Malla, B. K.; Vishwakarma, G.; Nyayban, A.; Pradeep, T. Composition-Dependent Formation and Dissociation of Structure I and Structure II Clathrate Hydrates of Trimethylene Oxide in Ultrahigh Vacuum. *J. Phys. Chem. C* **2025**, *129* (19), 8937−8945.

(26) Malla, B. K.; Yang, D.; Pradeep, T. Growth of Clathrate Hydrates in Nanoscale Ice Films Observed Using Electron Diffraction and Infrared Spectroscopy. *J. Phys. Chem. Lett.* **2025**, *16* (1), 365−371.

(27) Charnley, S. B. Acetaldehyde in Star-Forming Regions. *Adv. Sp. Res.* **2004**, *33* (1), 23−30.

(28) Matthews, H. E.; Friber, P.; Irvine, W. M. The Detection of Acetaldehyde in Cold Dust Clouds. *Astrophys. J.* **1985**, *290*, 609.

https://doi.org/10.1021/acs.jpclett.6c00885
J. Phys. Chem. Lett. XXXX, XXX, XXX−XXX

(29) Kleimeier, N. F.; Turner, A. M.; Fortenberry, R. C.; Kaiser, R. I. On the Formation of the Popcorn Flavorant 2,3-Butanedione (CH3COCOCH3) in Acetaldehyde-Containing Interstellar Ices. *ChemPhysChem* **2020**, *21* (14), 1531−1540.
(30) Gibb, E. L.; Whittet, D. C. B.; Boogert, A. C. A.; Tielens, A. G. G. M. Interstellar Ice: The Infrared Space Observatory Legacy. *Astrophys. J. Suppl. Ser.* **2004**, *151* (1), 35−73.
(31) Bag, S.; Bhuin, R. G.; Methikkalam, R. R. J.; Pradeep, T.; Kephart, L.; Walker, J.; Kuchta, K.; Martin, D.; Wei, J. Development of Ultralow Energy (1−10 EV) Ion Scattering Spectrometry Coupled with Reflection Absorption Infrared Spectroscopy and Temperature Programmed Desorption for the Investigation of Molecular Solids. *Rev. Sci. Instrum.* **2014**, *85* (1), 14103.
(32) Vishwakarma, G.; Malla, B. K.; Kumar, R.; Pradeep, T. Partitioning Photochemically Formed CO2 into Clathrate Hydrate under Interstellar Conditions. *Phys. Chem. Chem. Phys.* **2024**, *26* (22), 16008−16016.
(33) Takeya, K.; Tani, A.; Yada, T.; Ikeya, M.; Ohgaki, K. Electron Spin Resonance Study on γ-Ray-Induced Methyl Radicals in Methane Hydrates. *Jpn. J. Appl. Phys.* **2004**, *43* (1), 353−357.
(34) Ohgaki, K.; Nakatsuji, K.; Takeya, K.; Tani, A.; Sugahara, T. Hydrogen Transfer from Guest Molecule to Radical in Adjacent Hydrate-Cages. *Phys. Chem. Chem. Phys.* **2008**, *10* (1), 80−82.
(35) Sugahara, T.; Kobayashi, Y.; Tani, A.; Inoue, T.; Ohgaki, K. Intermolecular Hydrogen Transfer between Guest Species in Small and Large Cages of Methane + Propane Mixed Gas Hydrates. *J. Phys. Chem. A* **2012**, *116* (10), 2405−2408.
(36) Vishwakarma, G.; Malla, B. K.; Chowdhury, S.; Ghosh, J.; Methikkalam, R. R. J.; Kumar, R.; Pradeep, T. Ultraviolet Photolysis of CO2 Clathrate Hydrate and H2O−CO2Mixed Ice under Ultrahigh Vacuum. *Phys. Chem. Chem. Phys.* **2025**, *27* (21), 11025−11035.
(37) Malla, B. K.; Chowdhury, S.; Bhardwaj, K.; Kumar, R.; Pradeep, T. Water Cages as Chemical Reactors: VUV Photolysis of Dimethyl Ether Clathrate Hydrate Thin Films in Ultrahigh Vacuum. *J. Phys. Chem. Lett.* **2026**, *17*, 3662.
(38) Gerakines, P. A.; Schutte, W. A.; Greenberg, J. M.; van Dishoeck, E. F. The Infrared Band Strengths of H2O, CO and CO2 in Laboratory Simulations of Astrophysical Ice Mixtures. *Astron. Astrophys.* **1995**, *296* (3), 810−818.
(39) Martín-Doménech, R.; Muñoz Caro, G. M.; Cruz-Díaz, G. A. Study of the Photon-Induced Formation and Subsequent Desorption of CH3OH and H2CO in Interstellar Ice Analogs. *Astron. Astrophys.* **2016**, *589*, A107−A107.
(40) Bouilloud, M.; Fray, N.; Bénilan, Y.; Cottin, H.; Gazeau, M.-C.; Jolly, A. Bibliographic Review and New Measurements of the Infrared Band Strengths of Pure Molecules at 25 K: H2O, CO2, CO, CH4, NH3, CH3OH, HCOOH and H2CO. *Mon. Not. R. Astron. Soc.* **2015**, *451* (2), 2145−2160.
(41) Milligan, D. E.; Jacox, M. E. Infrared Spectrum and Structure of Intermediates in the Reaction of OH with CO. *J. Chem. Phys.* **1971**, *54* (3), 927−942.
(42) Morley, C.; Smith, I. W. M. Rate Measurements of Reactions of OH by Resonance Absorption. Part 1.—Reactions of OH with NO 2 and NO. *J. Chem. Soc., Faraday Trans. 2* **1972**, *68*, 1016−1030.
(43) Terwisscha Van Scheltinga, J.; Ligterink, N. F. W. W.; Boogert, A. C. A. A.; Van Dishoeck, E. F.; Linnartz, H. Infrared Spectra of Complex Organic Molecules in Astronomically Relevant Ice Matrices: I. Acetaldehyde, Ethanol, and Dimethyl Ether. *Astron. Astrophys.* **2018**, *611*, A35−A35.
(44) Öberg, K. I.; Garrod, R. T.; van Dishoeck, E. F.; Linnartz, H. Formation Rates of Complex Organics in UV Irradiated CH3OH-Rich Ices. *Astron. Astrophys.* **2009**, *504* (3), 891−913.
(45) Butscher, T.; Duvernay, F.; Danger, G.; Chiavassa, T. Radical-Induced Chemistry from VUV Photolysis of Interstellar Ice Analogues Containing Formaldehyde. *Astron. Astrophys.* **2016**, *593*, A60−A60.
(46) Hudson, R. L.; Loeffler, M. J. Ketene Formation in Interstellar ICES: A Laboratory Study. *Astrophys. J.* **2013**, *773* (2), 109.
(47) Hudson, R. L.; Ferrante, R. F. Quantifying Acetaldehyde in Astronomical Ices and Laboratory Analogues: IR Spectra, Intensities, 13C Shifts, and Radiation Chemistry. *Mon. Not. R. Astron. Soc.* **2020**, *492* (1), 283−293.
(48) Jacox, M. E.; Milligan, D. E. Matrix Isolation Study of the Vacuum-Ultraviolet Photolysis of Methanol. *J. Mol. Spectrosc.* **1973**, *47* (1), 148−162.
(49) Müller, B.; Giuliano, B. M.; Goto, M.; Caselli, P. Spectroscopic Measurements of CH3OH in Layered and Mixed Interstellar Ice Analogues. *Astron. Astrophys.* **2021**, *652*, A126−A126.
(50) Watanabe, N.; Kouchi, A. Ice Surface Reactions: A Key to Chemical Evolution in Space. *Prog. Surf. Sci.* **2008**, *83* (10−12), 439−489.
(51) Bisschop, S. E.; Fuchs, G. W.; Van Dishoeck, E. F.; Linnartz, H. H-Atom Bombardment of CO2, HCOOH, and CH3CHO Containing Ices. *Astron. Astrophys.* **2007**, *474* (3), 1061−1071.
(52) Chuang, K.-J.; Fedoseev, G.; Qasim, D.; Ioppolo, S.; Jäger, C.; Henning, T.; Palumbo, M. E.; Van Dishoeck, E. F.; Linnartz, H. Formation of Complex Molecules in Translucent Clouds: Acetaldehyde, Vinyl Alcohol, Ketene, and Ethanol via "Nonenergetic" Processing of C2H2 Ice. *Astron. Astrophys.* **2020**, *635*, A199.
(53) Mondal, S. K.; Gorai, P.; Sil, M.; Ghosh, R.; Etim, E. E.; Chakrabarti, S. K.; Shimonishi, T.; Nakatani, N.; Furuya, K.; Tan, J. C.; Das, A. Is There Any Linkage between Interstellar Aldehyde and Alcohol? *Astrophys. J.* **2021**, *922* (2), 194.
(54) Zasimov, P. V.; Sanochkina, E. V.; Feldman, V. I. Radiation-Induced Transformations of Acetaldehyde Molecules at Cryogenic Temperatures: A Matrix Isolation Study. *Phys. Chem. Chem. Phys.* **2021**, *24* (1), 419−432.
(55) Zasimov, P. V.; Volosatova, A. D.; Góbi, S.; Keresztes, B.; Tyurin, D. A.; Feldman, V. I.; Tarczay, G. Infrared Spectroscopy of the α-Hydroxyethyl Radical Isolated in Cryogenic Solid Media. *J. Chem. Phys.* **2024**, *160* (2), No. 024308.
(56) Molpeceres, G.; Nguyen, T.; Oba, Y.; Watanabe, N. Hydrogenation of Acetaldehyde on Interstellar Ice Analogs Results in Limited Destruction. *Astron. Astrophys.* **2025**, *694*, A299.
(57) Rocha, W. R. M.; van Dishoeck, E. F.; Ressler, M. E.; van Gelder, M. L.; Slavicinska, K.; Brunken, N. G. C.; Linnartz, H.; Ray, T. P.; Beuther, H.; Caratti o Garatti, A.; Geers, V.; Kavanagh, P. J.; Klaassen, P. D.; Justtanont, K.; Chen, Y.; Francis, L.; Gieser, C.; Perotti, G.; Tychoniec, Ł.; Barsony, M.; Majumdar, L.; le Gouellec, V. J. M.; Chu, L. E. U.; Lew, B. W. P.; Henning, T.; Wright, G. JWST Observations of Young ProtoStars (JOYS+): Detecting Icy Complex Organic Molecules and Ions. *Astron. Astrophys.* **2024**, *683*, A124−A124.
(58) Watanabe, N.; Kouchi, A. Efficient Formation of Formaldehyde and Methanol by the Addition of Hydrogen Atoms to CO in H2O-CO Ice at 10 K. *Astrophys. J.* **2002**, *571* (2), L173−L176.
(59) Escribano, R. M.; Muñoz Caro, G. M.; Cruz-Diaz, G. A.; Rodríguez-Lazcano, Y.; Maté, B. Crystallization of CO2 Ice and the Absence of Amorphous CO2 Ice in Space. *Proc. Natl. Acad. Sci. U.S.A.* **2013**, *110* (32), 12899−12904.
(60) Fleyfel, F.; Devlin, J. P. FT-IR Spectra of 90 K Films of Simple, Mixed, and Double Clathrate Hydrates of Trimethylene Oxide, Methyl Chloride, Carbon Dioxide, Tetrahydrofuran, and Ethylene Oxide Containing Decoupled D2O. *J. Phys. Chem.* **1988**, *92* (3), 631−635.
(61) Fleyfel, F.; Devlin, J. P. Carbon Dioxide Clathrate Hydrate Epitaxial Growth: Spectroscopic Evidence for Formation of the Simple Type-II Carbon Dioxide Hydrate. *J. Phys. Chem.* **1991**, *95* (9), 3811−3815.
(62) Netsu, R.; Ikeda-Fukazawa, T. Formation of Carbon Dioxide Clathrate Hydrate from Amorphous Ice with Warming. *Chem. Phys. Lett.* **2019**, *716*, 22−27.
(63) Limão-Vieira, P.; Eden, S.; Mason, N. J.; Hoffmann, S. V. Electronic State Spectroscopy of Acetaldehyde, CH3CHO, by High-Resolution VUV Photo-Absorption. *Chem. Phys. Lett.* **2003**, *376* (5−6), 737−747.

https://doi.org/10.1021/acs.jpclett.6c00885
J. Phys. Chem. Lett. XXXX, XXX, XXX−XXX